

Physical ageing and molecular mobility in PLA blends and composites

Péter Müller^{1,2} · Balázs Imre^{1,2} · József Bere^{1,2} ·
János Móczó^{1,2} · Béla Pukánszky^{1,2}

Received: 8 January 2015 / Accepted: 2 June 2015 / Published online: 2 July 2015
© Akadémiai Kiadó, Budapest, Hungary 2015

Abstract Poly(lactic acid) (PLA) blends and composites were prepared from thermoplastic starch, poly(butylene-adipate-co-terephthalate), polycarbonate, wood flour and CaSO₄ in a wide range of compositions. The thermal transitions of PLA were studied by differential scanning calorimetry. The detailed analysis of the transitions of PLA/thermoplastic starch blends indicated that they all are determined by the molecular mobility of PLA chains. Blending changes molecular mobility, and thus it often decreases glass transition temperature and modifies the extent of enthalpy relaxation. All other transitions and characteristics, i.e. cold crystallization, melting and the corresponding enthalpies, change accordingly. Increased molecular mobility accelerates also the physical ageing of the polymer. The interaction between PLA and the various components used for modification changed in a wide range, but no direct correlation was found between the strength of interaction and molecular mobility.

Keywords PLA · Blends · Composites · Thermal transitions · DSC · Molecular mobility · Physical ageing

Introduction

PLA has created much interest recently, because of the combination of its biodegradability with numerous advantageous properties. PLA is produced from renewable resource [1], and the increase in production capacity lowered its price to reasonable levels. The polymer is used in increasing quantities for various applications in several fields including packaging [2, 3], consumer goods [2] and the electronic and automotive industries [2, 4]. However, besides its advantages, PLA also has several drawbacks. Its slow crystallization [5, 6] and fast physical ageing [7, 8] result in unstable structure and rapidly changing properties, which might result in brittleness, fast deterioration of properties and finally catastrophic failure. As a consequence, PLA is often modified by various means including copolymerization [9–11], plasticization [12–14], blending [15, 16], incorporation of various fillers [17–20] and reinforcements [21–23]. These components modify all properties of the polymer, often in an unpredictable manner; contradictory results are reported on the effect of such modifications in the literature.

Similar to other polyesters, PLA crystallizes relatively slowly [5, 6]. Most products prepared by traditional melt-processing technologies are amorphous as a result [24], although the properties of crystalline PLA might be more advantageous in several respects [25]. Occasionally, partially crystalline parts can be also produced depending on processing conditions and composition. Because of the importance of crystallinity and crystalline structure in the determination of properties, a very large number of studies have been dedicated to their investigation, and many attempts have been made to modify them [6, 26–30]. However, the determination of unambiguous correlations between crystallization conditions, composition and

✉ János Móczó
jmoczo@mail.bme.hu

¹ Laboratory of Plastics and Rubber Technology, Department of Physical Chemistry and Materials Science, Budapest University of Technology and Economics, P.O. Box 91, Budapest 1521, Hungary

² Institute of Materials and Environmental Chemistry, Chemical Research Center, Hungarian Academy of Sciences, P.O. Box 286, Budapest 1519, Hungary

structure is difficult because of the complicated structure and many transitions appearing on the DSC trace of PLA. During the heating of amorphous PLA, the polymer goes through glass transition first (T_g), and then cold crystallization (T_{cc} , ΔH_{cc}) occurs. The crystals formed in the latter process melt at higher temperature (T_m , ΔH_m). PLA can crystallize in α , α' , β and γ forms [6], and crystal perfection, recrystallization and change of modification may result in multiple peaks during heating and sometimes also during crystallization [6]. Even the amorphous phase of semicrystalline PLA has a complicated structure; it is claimed to contain three types of amorphous molecules: the rigid amorphous fraction, the interspherulitic mobile amorphous phase and the intraspherulitic mobile amorphous phase [31].

Attempts have been made to modify the crystalline structure by nucleation. Talc was claimed to nucleate PLA efficiently [5, 32–35], and the combination of the filler with organic compounds was said to improve crystallization characteristics, i.e. nucleus density and crystalline growth rate [32, 36]. However, the results are often ambiguous and contradictory. Difficulties of interpretation are further increased by the fact that the nucleation efficiency of a certain substance is sometimes evaluated by its effect on the temperature of cold crystallization [19, 27–29, 37–40], while in other cases by cooling from a quiescent melt [34, 35, 41]. Crystallization can be accelerated also by the use of plasticizers [5, 12–14, 42–44] which increase the mobility of PLA chains. Often this approach and effect are also called nucleation [44].

The addition of another polymer, i.e. blending, or the use of fillers or reinforcements further complicates this complex picture. For example, the incorporation of organophilic clay increased T_g in one case [38], decreased it in another [29], while glass transition temperature remained constant in a third [39]. The same can be said about all crystallization characteristics including the temperature and enthalpy of cold crystallization, melting or crystallization and about the effect of all kinds of additional components including plasticizers, elastomers, polymers, fillers [5, 12, 27, 39, 45–49].

Blending PLA with other biodegradable polymers like TPS might result in cost reduction while maintaining or enhancing its biodegradability. In spite of the large number of publications dealing with PLA/TPS blends, only a few studies are available on the crystallization and melting behaviour of the these blends. Most of the authors claim progressive melting, glass transition and cold crystallization temperature decrease with increasing TPS content [13, 50], while others report that glass transition temperature remains constant [51]. In these blends, the plasticizer content of TPS can migrate into the PLA, increasing chain mobility, which leads to increased crystalline growth rate

[52, 53]. Because of the simultaneous effect of nucleation and molecular mobility, the clear effect of the additive is difficult to define. Since physical ageing also affects molecular mobility and thus crystallization, this process influences practically all characteristics determined by thermoanalytical methods. Moreover, time and thermal history also play a role, a factor which is neglected in most experiments.

In a series of experiments, we prepared poly(lactic acid)/thermoplastic starch blends in the entire composition range to determine the effect of composition on properties. DSC measurements yielded interesting results which were difficult to explain. In order to be able to interpret the results better and to draw general conclusions, if possible, the results obtained on PLA/TPS blends were compared to other heterogeneous PLA blends (PBAT, PC) and composites (CaSO₄, wood). This paper reports the most important results and conclusions of these studies, during the interpretation of which also the effect of physical ageing was considered.

Experimental

Materials

The PLA used as matrix was obtained from NatureWorks (USA). The selected grade (Ingeo 4032D, $M_n = 88,500 \text{ g mol}^{-1}$ and $M_w/M_n = 1.8$) is recommended for extrusion. The polymer (<2 % D isomer) has a density of 1.24 g cm^{-3} , while its melt flow index (MFI) is $3.9 \text{ g } 10 \text{ min}^{-1}$ at $190 \text{ }^\circ\text{C}$ and 2.16 kg load. The corn starch used for the preparation of TPS was supplied by Hungrana Ltd., Hungary, and its water content was 12 mass%. Glycerol with 0.5 mass% water content was obtained from Molar Chemicals Ltd., Hungary, and it was used for the plasticization of starch without further purification or drying. Thermoplastic starch samples containing 36 and 47 mass% glycerol (TPS36 and TPS47, respectively) were prepared and used in the experiments. The composition of the PLA/TPS blends changed from 0 to 1 volume fraction in 0.1 volume fraction steps. Glycerol was added to PLA also in itself as a “plasticizer” in 1, 3, 5, 7 and 10 vol%.

Polycarbonate (Macrolon 2658, Bayer Material Science AG, MFI = $13 \text{ g } 10 \text{ min}^{-1}$ at $300 \text{ }^\circ\text{C}$, 1.2 kg, density = 1.2 g cm^{-3}) and poly(butylene-adipate-co-terephthalate) (Ecoflex F BX 7011, BASF, MFI = $3.5 \text{ g } 10 \text{ min}^{-1}$ at $190 \text{ }^\circ\text{C}$, 2.16 kg, density = 1.26 g cm^{-3}) were used as blend components. Compositions covered the entire composition ranging from 0 to 1 volume fraction in 0.1 volume fraction steps.

Five different lignocellulosic fibres were used as reinforcement, three wood flours (W), a microcrystalline

cellulose (MC) and a ground corn cob (CC). Two of the wood flours, Filtracel EFC 1000 (W68, $D[4,3] = 213.1 \mu\text{m}$, aspect ratio, $AR = 6.8$) and Arbocel FT400 (W126, $D[4,3] = 171.0 \mu\text{m}$, $AR = 12.6$), were acquired from Rettenmaier und Söhne GmbH, Germany, while the third, Lasole 200/150 (W54, $D[4,3] = 280.8 \mu\text{m}$, $AR = 5.4$) from La.So.Le. Est Srl, Italy. All three were soft woods; further information was not supplied by the producer. The microcrystalline cellulose, Vivapur MCC (MC29, $D[4,3] = 138.0 \mu\text{m}$, $AR = 2.9$), was acquired from Rettenmaier und Söhne GmbH, Germany. The fifth filler was the heavy fraction of corn cob (CC, $D[4,3] = 143.4 \mu\text{m}$, $AR = 2.3$) obtained from Boly Kft., Hungary. Particle size $D[4,3]$ was determined by laser light scattering, while aspect ratio (AR) manually from SEM micrographs. The abbreviation used indicates the origin of the fibres (wood, W; microcrystalline cellulose, MC; or corn cob, CC) and ten times their aspect ratio, i.e. corn cob with an aspect ratio of 2.3 is referred to as CC23. The amount of the reinforcement usually changed from 0 to 60 mass%, but sometimes composites could not be processed with the largest fibre content because of technological reasons.

The CAS-20-4 calcium sulphate (CaSO_4) used as filler was supplied by the United States Gypsum Co. (USA). The filler, manufactured from high-purity gypsum rock using controlled calcination and fine grinding, has a volume-average particle size of $4.4 \mu\text{m}$, specific gravity of 2.96 g cm^{-3} and calcium sulphate content $>99 \%$. The filler was surface coated with 1.5 mass% stearic acid, $\text{CaSO}_4(\text{StAc})$, resulting in monolayer coverage [28] in order to modify interfacial interactions. Coating was carried out at $120 \text{ }^\circ\text{C}$ and 100 rpm for 10 min in a Haake Rheomix 600 mixer fitted with blades for dry-blending. The CaSO_4 content of PLA composites, both with coated and uncoated fillers, was changed from 0 to 30 vol% in 5 vol% steps.

Sample preparation

Corn starch was dried in an oven before composite preparation ($105 \text{ }^\circ\text{C}$, 24 h). Thermoplastic starch powder containing 36 and 47 mass% glycerol was prepared by dry-blending in a Henschel FM/A10 high-speed mixer at 2000 rpm. TPS was produced by processing the dry blend in a Rheomex 3/4" single-screw extruder attached to a Haake Rheocord EU 10-V driving unit at $140\text{--}150\text{--}160 \text{ }^\circ\text{C}$ barrel and $170 \text{ }^\circ\text{C}$ die temperatures and 60-rpm screw speed.

PLA and the second component were homogenized in an internal mixer (Brabender W 50 EHT) at $190 \text{ }^\circ\text{C}$ and 50 rpm for 12 min. Before composite preparation, poly(lactic acid) was dried in a vacuum oven ($110 \text{ }^\circ\text{C}$, 4 h).

The wood fibres and the polymers (PBAT, PC) were dried in an oven ($105 \text{ }^\circ\text{C}$, 4 h, $80 \text{ }^\circ\text{C}$, 4 h and $120 \text{ }^\circ\text{C}$, 3 h, respectively) before processing. Both temperature and torque were recorded during homogenization. The melt was transferred to a Fontijne SRA 100 compression moulding machine ($190 \text{ }^\circ\text{C}$, 5 min) to produce 1-mm-thick plates for further testing.

To study the effect of physical ageing on the mechanical properties of PLA, standard specimens (ISO 527 1A) were produced by injection moulding (Demag IntElect 50/330-100) at $180\text{--}190\text{--}200\text{--}210 \text{ }^\circ\text{C}$ barrel and $20 \text{ }^\circ\text{C}$ mould temperature, using 900 bar injection and 700 bar holding pressure (decreasing to 0 bar in 40 s), after drying the polymer according to the procedure described above. All specimens were kept in a room with controlled temperature and humidity ($23 \text{ }^\circ\text{C}$ and 50 %) after injection moulding.

Characterization

Thermal transitions including glass transition, melting and crystallization of the blends and composites prepared were studied by differential scanning calorimetry (DSC) using a PerkinElmer DSC 7 equipment. Three to five milligrams of samples was heated to $200 \text{ }^\circ\text{C}$ at $10 \text{ }^\circ\text{C min}^{-1}$ heating rate, kept there for 5 min to erase thermal history and then cooled down to $50 \text{ }^\circ\text{C}$ with $5 \text{ }^\circ\text{C min}^{-1}$ cooling rate to record crystallization characteristics. After 1-min holding time, the samples were heated again to $200 \text{ }^\circ\text{C}$ at $10 \text{ }^\circ\text{C min}^{-1}$ rate to determine the same thermal characteristics as in the first run.

The effect of physical ageing of PLA on its mechanical properties was followed by tensile testing on standard 4-mm-thick ISO 527 1A specimens using an Instron 5566 apparatus. Stiffness (E) was determined at 0.5 mm/min cross-head speed (up to 0.3 % elongation) and 115-mm gauge length. Tensile strength (σ) and elongation at break (ϵ) were calculated from force versus deformation traces measured on the same specimens at 10 mm min^{-1} cross-head speed.

Results and discussion

The results are reported in several sections. The thermal behaviour of PLA/TPS blends is presented first, and then the possible role of glycerol is discussed in the next section. The results obtained on starch blends are compared to those determined on other blends and composites subsequently, while the possible role of physical ageing in the determination of thermal transitions, including crystallization, is discussed in the final section.

PLA/TPS blends

PLA is frequently modified with thermoplastic starch in order to decrease the brittleness of the polymer, to increase impact resistance and to facilitate biodegradation [50, 54–57]. The mechanical properties of the blends change accordingly, stiffness decreases and deformability increases with increasing TPS content [13, 50, 51, 57, 58]. DSC traces recorded in the first heating run on PLA blends prepared with the TPS containing 36 mass% glycerol (TPS36) are presented in Fig. 1. The comparison of the traces obtained at various TPS levels offers some information. The glass transition temperature of PLA does not seem to change, or it may increase slightly as a function of TPS content. It is even more interesting that the intensity of the transition varies strongly. A distinct peak corresponding to the glass transition appears at 20 vol%, and similar peaks can be observed also at higher concentrations of TPS except at 60 vol%. The dissimilar behaviour of this blend is difficult to explain, but it is in line with the sometimes unpredictable behaviour of PLA blends and composites [28]. The distinct peak detected at glass transition results from the physical ageing of PLA. These changes in the glass transition process of the polymer indicate that blending might influence its physical ageing and modify the state of the molecules compared with their equilibrium state.

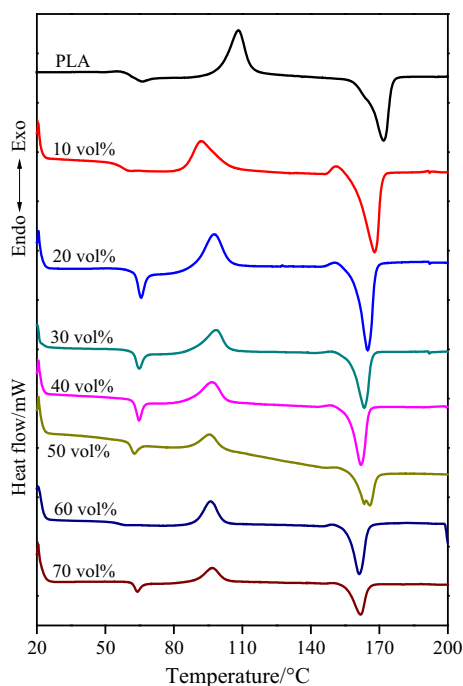


Fig. 1 DSC traces recorded during the first heating run on PLA/TPS36 blends. Effect of TPS content

Considerable changes can be observed in the other transitions as well. The temperature of cold crystallization definitely moves towards lower temperatures. Possible changes in intensity are difficult to estimate by the qualitative observation of the traces; quantitative analysis is needed. Similarly, changes can be observed in the temperature range of melting as well. First a small exothermic peak or shoulder appears in the trace, and then the crystalline polymer melts [35, 59]. The peak temperature of fusion moves towards lower temperatures with increasing TPS content, but compared to the neat polymer, its intensity increases visibly indicating larger crystallinity in the blends. Obviously, blending with thermoplastic starch profoundly changes the thermal behaviour of PLA; all transitions are modified from glass transition through cold crystallization to melting. TPS seems to change the mobility of PLA molecules thus modifying physical ageing and crystallization.

DSC traces obtained during the cooling of the polymer from the quiescent melt state are shown in Fig. 2. The strong effect of TPS is seen clearly in the figure. PLA crystallizes very slowly, and only a small undefined peak appears on the DSC trace. The intensity of the crystallization peak increases with increasing TPS content; the phenomenon is demonstrated well by the trace obtained on the blend containing 20 vol% TPS36. Double peaks appear on most of the traces, which might result from the formation of

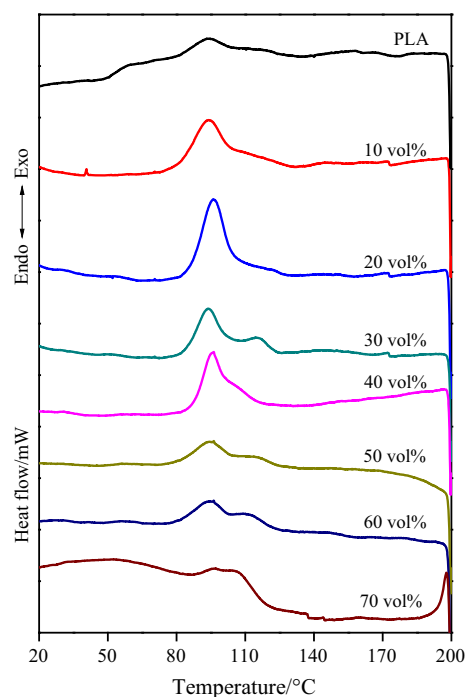


Fig. 2 Effect of TPS content on the crystallization of PLA in the PLA/TPS blends of Fig. 1

various modifications [6]. Different crystalline structures have been reported for PLA, the formation of which depends on the conditions of crystallization. The most common α -modification forms in conventional melt and solution crystallization conditions. However, only the α' crystal appears at crystallization temperatures below 100 °C, while crystallization between 100 and 120 °C results in the simultaneous formation of the α' and the α crystal structures [59, 60]. The β and the γ modifications occur under more special conditions, the first during the orientation of the α form, while the second through epitaxial crystallization. We may safely assume that under the conditions of our experiments, first the less perfect α' form develops, which recrystallizes during heating to the more ordered α form. However, further study is needed to explain the appearance of multiple peaks unambiguously and relate them to structure. Such change of the melting process is usually explained by nucleation. However, the temperature of crystallization seems to remain the same or changes only slightly, and thus increased crystallinity must result from increased molecular mobility thus supporting our earlier assumption.

The qualitative analysis presented above is strongly supported by quantitative evaluation. The glass transition temperature of the two sets of blends is plotted against TPS content in Fig. 3. T_g increases slightly as deduced from the primary DSC traces. The values are very similar for the two series; the glycerol content of TPS does not seem to influence them much. We can see several points deviating from the general tendency. Such behaviour was observed in PLA/CaSO₄ blends before [28], for which a clear and unambiguous explanation could not be given. Even the increasing glass transition temperature of PLA is difficult to explain, since the T_g of the two TPS materials is 10 and 40 °C, respectively, and thus a decrease in PLA T_g would

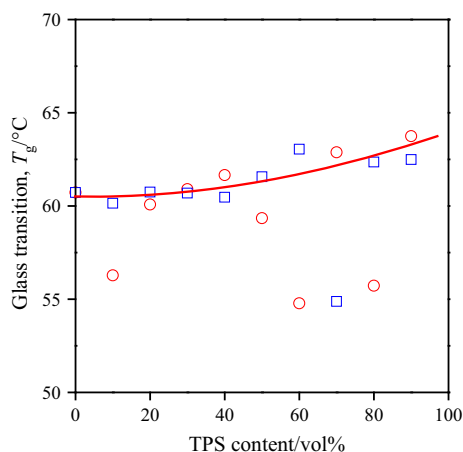


Fig. 3 Effect of TPS content on the glass transition temperature of PLA in PLA/TPS blends. Symbols: ○ TPS36, □ TPS47

be expected instead the increase observed. Both the unexpected change in T_g and the large scatter of some experimental values must be related to the physical state of PLA not controlled sufficiently by experimental conditions.

The composition dependence of the temperature of cold crystallization is presented in Fig. 4 for both series of blends. The figure confirms the qualitative observation that T_{cc} decreases with increasing TPS content. The decrease is very similar for the two series independently of glycerol content. The plot contains several deviating points again, which seems to be a typical characteristic of PLA irrespective of composition or the quantity investigated. Melting characteristics determined in the first heating run are shown in Fig. 5. The results corroborate our previous statements and conclusions even stronger than Figs. 3 and 4. The temperature of fusion decreases strongly with increasing TPS content, while crystallinity increases at the same time. The composition dependence of thermal characteristics seems to support our assumption that these changes result from the modification of molecular mobility of PLA, which changes upon blending. Since the temperature of crystallization remains constant (not shown), they cannot result from nucleation. Although the facts are clear, the explanation is still missing. Since glycerol is a polar molecule and PLA is also capable of forming hydrogen bonds, the possible effect of glycerol must be considered specifically.

PLA/glycerol blends

Since our primary assumption is that modification changes the mobility of PLA molecules, we must analyse the possible influence of glycerol on the thermal transitions of the polymer. As mentioned in the introductory part, plasticization is frequently used for the modification of PLA crystallization and crystalline structure [5, 6, 12–14, 42–44]. We refrain

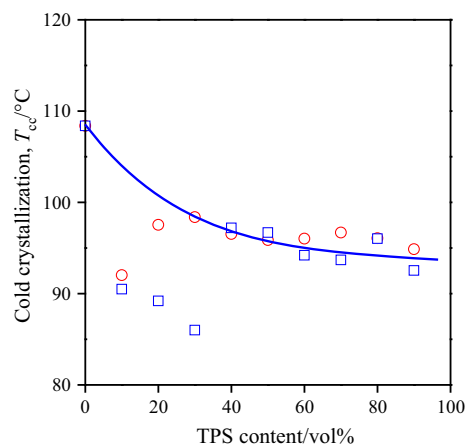


Fig. 4 Peak temperature of cold crystallization plotted against the TPS content of PLA/TPS blends. Symbols: ○ TPS36, □ TPS47

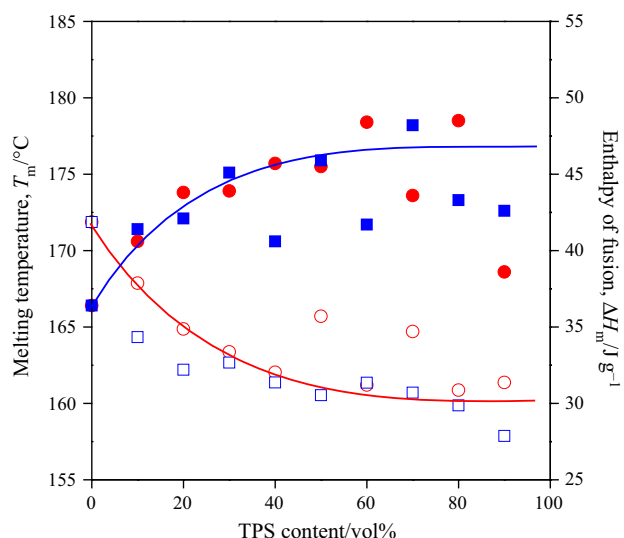


Fig. 5 Dependence of melting characteristics of PLA on TPS content. First heating run. Symbols: (○, ●) TPS36, (□, ■) TPS47; (○, □) peak temperature of melting, T_m , (●, ■) enthalpy of fusion, ΔH_m

from presenting all DSC traces and characteristic values and show only a few typical ones which can be evaluated in comparison with the previous section. Figure 6 shows the crystallization traces of PLA containing various amounts of glycerol. The traces are very similar to those presented in Fig. 2. Glycerol clearly enhances the rate of crystallization

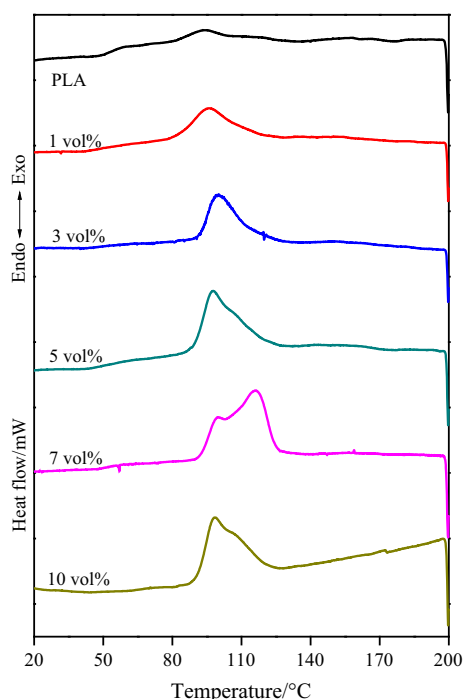


Fig. 6 DSC traces recorded during the cooling of PLA containing various amounts of glycerol

and crystallinity. The “plasticizer” has the same effect on glass transition temperature and melting characteristics as well; in fact the composition dependence of characteristic values changes in the same way as shown in Figs. 3–5 for PLA/TPS blends. An example is presented in Fig. 7, in which we plotted the peak temperature of melting and the heat of fusion as a function of glycerol content. The first decreases, while the second increases with increasing amount of the plasticizer, just like in the case of the TPS blends.

From the two figures and the results presented above, one may conclude that glycerol plasticizes PLA thus increasing molecular mobility, which finally leads to the changes observed. However, we must consider several facts here. First of all, the effect is completely independent of the glycerol content of TPS. Moreover, the solubility of glycerol is very limited in PLA shown by the transparency of PLA plates containing various amounts of glycerol (Fig. 8). Transparency does not change up to 1 vol%, but decreases sharply above 4 vol%. The composition dependence of the characteristics plotted in Fig. 7 differ considerably from that presented in Fig. 8; melting temperature and the enthalpy of fusion change also above 7 vol% at which transparency is practically constant. The relatively poor solubility of glycerol in PLA is confirmed by preliminary molecular modelling calculations as well showing much stronger interactions between glycerol and starch, than between glycerol and PLA. Although some plasticizing effect of glycerol cannot be excluded, the changes presented in “PLA/TPS blends” and “PLA/glycerol blends” sections seem to be of more general character.

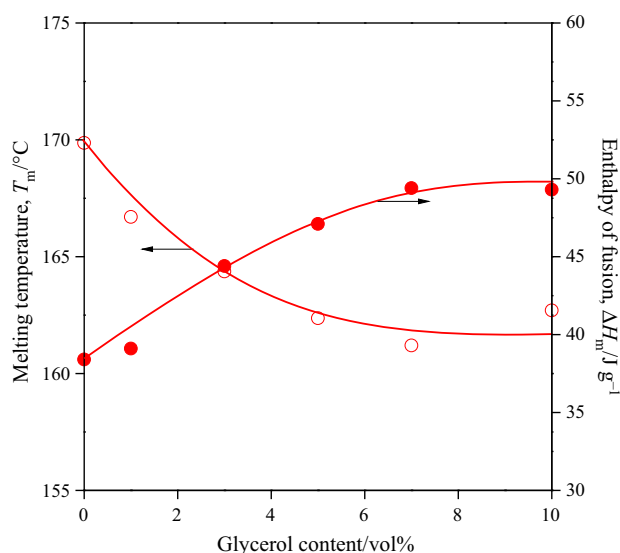


Fig. 7 Effect of glycerol content on the crystallization characteristics of PLA. Symbols: (○) peak temperature of crystallization, T_c , (●) enthalpy of crystallization, ΔH_c

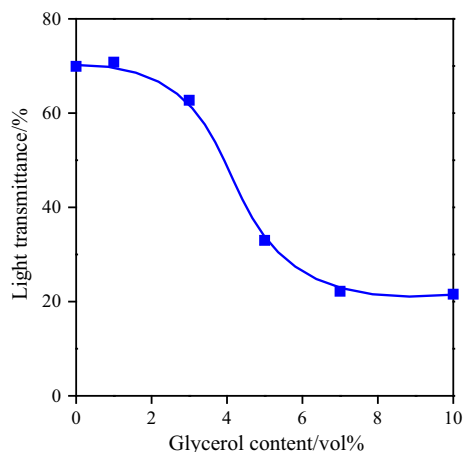


Fig. 8 Solubility of glycerol in PLA; effect of glycerol content on the transparency of 1-mm-thick PLA plates

Comparison, other blends and composites

Further blends and composites have been also prepared and studied at our laboratory; in order to increase the predictive power of our conclusions, DSC results have been compared for all of them. Selected crystallization traces are compared to each other in Fig. 9. Almost all combinations of materials result in the same effect as presented above irrespective of their type or quality. The dissimilar behaviour

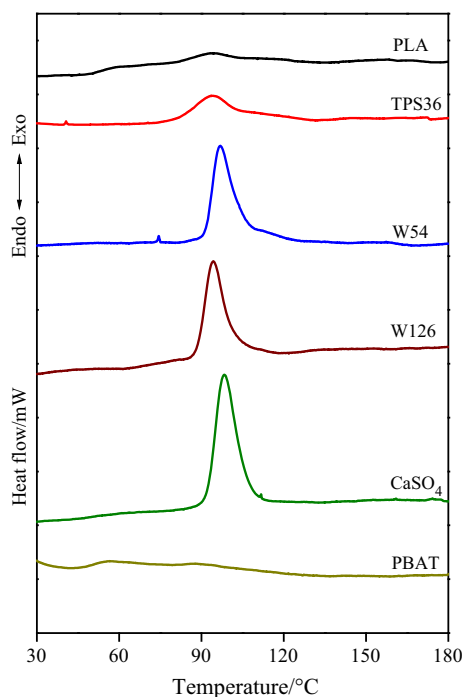


Fig. 9 Effect of various materials used for the modification of PLA on the crystallization of the matrix polymer in PLA blends and composites. The amount of the modifying component is 10 vol%

of PBAT is difficult to understand and needs further investigation. Practically every modification results in increased rate of crystallization and larger crystallinity. This result confirms our conclusion presented above that not glycerol specifically, but modification generally changes the thermal characteristics of PLA and the quantities derived from DSC measurements.

The glass transition temperature of PLA is plotted against the amount of selected materials used as second component in Fig. 10. T_g increases for the TPS blends, but decreases for all other materials. We could not explain the increase unambiguously, but the decrease is similarly difficult to understand, especially in the case of CaSO_4 having the highest surface energy. One would expect that PLA molecules adsorb onto the high-energy surface of the filler leading to decreased molecular mobility and increased glass transition temperature. Apparently thermal history and molecular mobility play more important roles in the determination of relaxation processes and glass transition than interactions. The correlation presented in Fig. 11 further confirms these relationships. The peak temperature of melting is plotted against composition for the same materials as in Fig. 10. T_m decreases for all materials irrespectively of their physical form or chemical composition indicating again easier crystallization kinetics caused mainly by increased mobility. The rest of the characteristics, i.e. the enthalpy of crystallization and fusion, change in the same way as presented in previous sections. The only difference in the effect of the materials used for modification is basically in the extent of the changes, which are influenced by undefined factors and must include ageing time, thermal history and probably also interactions.

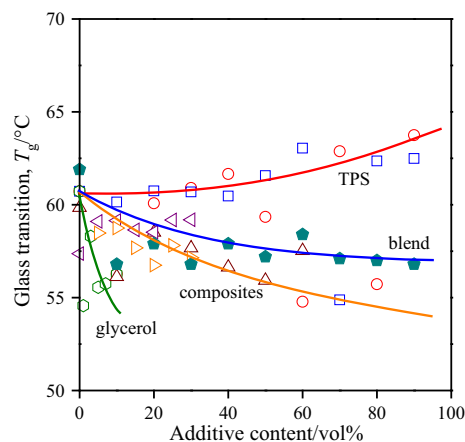


Fig. 10 Effect of modification on the glass transition temperature of PLA in various blends and composites. Symbols: (○) TPS36, (□) TPS 47, (●) glycerol, (△) W126, (◁) CaSO_4 , (▷) $\text{CaSO}_4(\text{StAc})$, (◆) PBAT

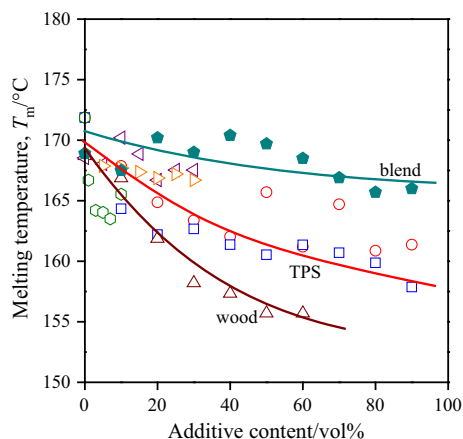


Fig. 11 Influence of the amount of the second component on the melting temperature of PLA blends and composites. Symbols are the same as in Fig. 10

Physical ageing and interactions

Physical ageing is a known disadvantage of PLA, which proceeds relatively fast because of the low glass transition temperature of the polymer and which results in considerable changes of properties in a relatively short time [7, 8, 19]. We discussed the possible effect of molecular mobility on the thermal transitions of PLA, and physical ageing is closely related to and depends on mobility. Figure 12 demonstrates the considerable modification of properties as an effect of physical ageing. Stiffness and deformability are plotted against ageing time in the figure. Modulus increases from about 2.7 to 3.2 GPa, while elongation at break decreases from more than 250 % to less than 10 %. This large

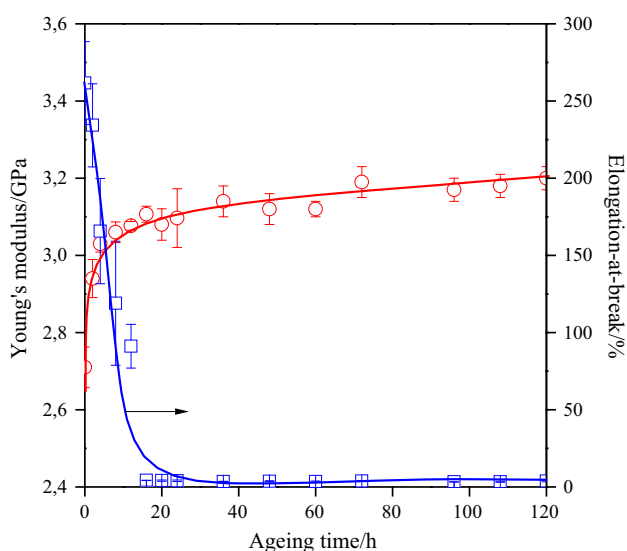


Fig. 12 Effect of ageing time on the mechanical properties of PLA. Symbols: (○) Young's modulus, (□) elongation at break

decrease in deformability results in the well-known brittleness of PLA that limits its application in certain fields.

The physical ageing process is accompanied by decreased T_g (Fig. 13), although the opposite effect, i.e. increased T_g was also observed by others [61]. The ageing process can be followed by the measurement of enthalpy relaxation; an endotherm peak appears at glass transition, the intensity of which increases with ageing time (Fig. 13). The peak is very similar to those shown in Fig. 1 during the glass transition of PLA, and thus we can safely assume that the modification of the polymer accelerates the ageing process by increasing mobility and bringing the molecules closer to their equilibrium state. All latter processes are determined by these changes, i.e. faster cold crystallization, larger crystallinity, less ordered crystals and lower melting temperature. Increased mobility is shown also by faster crystallization; nucleation has not been observed in our experiments indicated by the practically constant value of crystallization temperature (T_c).

Although the role of increased mobility and physical ageing seem to be rather certain, the reason is completely unclear and difficult to understand. PLA chains are rather flexible [62–64] shown also by the relatively low glass transition temperature of the polymer. Interactions between the molecules must be also quite weak since only van der Waals forces can develop among them, which is in line with the low T_g . One might expect strong interactions to develop between certain materials and PLA; it is able to form hydrogen bonds with starch and glycerol, for example, or adsorb onto the high-energy surface of inorganic fillers. The dispersion component of surface tension and the estimated reversible work of adhesion with PLA are listed

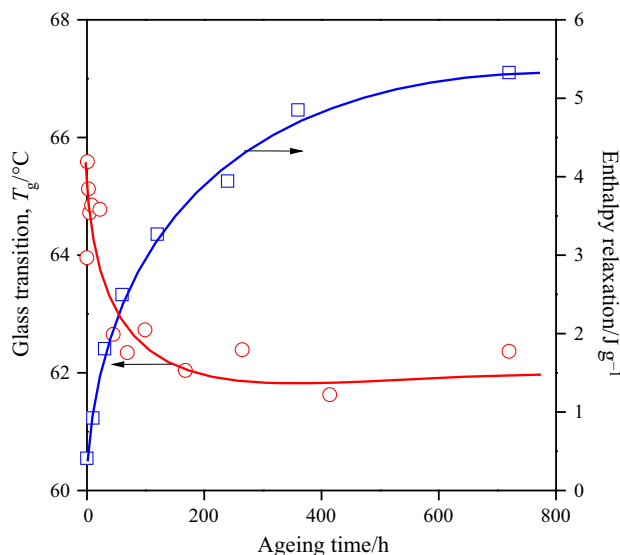


Fig. 13 Changes in glass transition temperature and the intensity of enthalpy relaxation during physical ageing. Symbols: (○) T_g , (□) enthalpy relaxation

Table 1 Surface energy of the second component and its estimated interfacial adhesion with PLA

Second component	Surface tension ^a , $\gamma_s^d/\text{mJ m}^{-2}$	Work of adhesion $W_a/\text{mJ m}^{-2}$
CaSO ₄	79.8	243.0
CaSO ₄ (StAc)	21.6	121.0
Wood	45.0	97.7
TPS	37.0	98.2

^a Dispersion component of surface tension

in Table 1 for selected materials. Interactions may play a role in the determination of the ageing process and molecular mobility, but it cannot be the determining factor. The T_g of PLA increased when TPS with small surface energy and weak interactions was added, while decreased when the filler having a surface with considerably higher energy was used for modification. More materials, further analysis and much more control of ageing history are needed in order to obtain the necessary correlations to control PLA properties sufficiently.

Conclusions

The detailed analysis of the transitions of PLA/thermoplastic starch blends indicated that all are determined by the molecular mobility of PLA chains. Blending modifies molecular mobility and thus often decreases glass transition temperature and changes the intensity of enthalpy relaxation. All other transitions and characteristics, i.e. cold crystallization, melting and the corresponding enthalpies, change accordingly. Increased molecular mobility accelerates also the physical ageing of the polymer. The comparison of the results to those obtained on other PLA blends (PBAT, PC) and composites (wood, CaSO₄) confirmed the general character of the phenomenon. Nucleation was not observed in the heterogeneous PLA blends and composites studied; crystallization temperature recorded during cooling from the quiescent melt remained constant. The interaction between PLA and the various components used for modification changed in a wide range, but no direct correlation was found between the strength of interaction and molecular mobility. The reason for the observed increase in mobility is unclear and needs further study and explanation.

Acknowledgements The authors are indebted to Zsolt László for his help in the determination of the particle characteristics of wood. The research on heterogeneous polymer systems was financed by the National Scientific Research Fund of Hungary (OTKA Grant No. K 101124) and by the Forbioplast FP7 project of EU (212239); we appreciate the support very much.

References

- Sawyer DJ. Bioprocessing—no longer a field of dreams. *Macromol Symp.* 2003;201:271–82.
- Ogawa S, Obuchi S. Packaging and other commercial applications. In: Auras R, Lim L-T, Selke SEM, Tsuji H, editors. *Poly(lactic acid): synthesis, structures, properties, processing, and applications.* Hoboken, New Jersey: Wiley; 2010. p. 457–67.
- Auras R, Harte B, Selke S. An overview of polylactides as packaging materials. *Macromol Biosci.* 2004;4:835–64.
- Ghosh SB, Bandyopadhyay-Ghosh S, Sain M. Composites. In: Auras R, Lim L-T, Selke SEM, Tsuji H, editors. *Poly(lactic acid).* Hoboken, New Jersey: Wiley; 2010. p. 293–310.
- Li H, Huneault MA. Effect of nucleation and plasticization on the crystallization of poly(lactic acid). *Polymer.* 2007;48:6855–66.
- Saeidlou S, Huneault MA, Li H, Park CB. Poly(lactic acid) crystallization. *Prog Polym Sci.* 2012;37:1657–77.
- Celli A, Scandola M. Thermal properties and physical ageing of poly(L-lactic acid). *Polymer.* 1992;33:2699–703.
- Kwon M, Lee S, Jeong Y. Influences of physical aging on enthalpy relaxation behavior, gas permeability, and dynamic mechanical property of polylactide films with various D-isomer contents. *Macromol Res.* 2010;18:346–51.
- Li B, Chen SC, Qiu ZC, Yang QKK, Tang SP, Yu WJ, Wang YZ. Synthesis of poly(lactic acid-*b-p*-dioxanone) block copolymers from ring opening polymerization of *p*-dioxanone by poly(L-lactic acid) macroinitiators. *Polym Bull.* 2008;61:139–46.
- Ho CH, Wang CH, Lin CI, Lee YD. Synthesis and characterization of TPO-PLA copolymer and its behavior as compatibilizer for PLA/TPO blends. *Polymer.* 2008;49:3902–10.
- Södergard A, Stolt M. Properties of lactic acid based polymers and their correlation with composition. *Prog Polym Sci.* 2002;27: 1123–63.
- Lemmouchi Y, Murariu M, Dos Santos AM, Amass AJ, Schacht E, Dubois P. Plasticization of poly(lactide) with blends of tributyl citrate and low molecular weight poly(D, L-lactide)-*b*-poly(ethylene glycol) copolymers. *Eur Polym J.* 2009;45:2839–48.
- Martin O, Averous L. Poly(lactic acid): plasticization and properties of biodegradable multiphase systems. *Polymer.* 2001;42: 6209–19.
- Ljungberg N, Wesslen B. Tributyl citrate oligomers as plasticizers for poly(lactic acid): thermo-mechanical film properties and aging. *Polymer.* 2003;44:7679–88.
- Gu SY, Zhang K, Ren J, Zhan H. Melt rheology of polylactide/poly(butylene adipate-co-terephthalate) blends. *Carbohydr Polym.* 2008;74:79–85.
- Rohman G, Laupretre F, Boileau S, Guerin P, Grande D. Poly(D, L-lactide)/poly(methyl methacrylate) interpenetrating polymer networks: synthesis, characterization, and use as precursors to porous polymeric materials. *Polymer.* 2007;48: 7017–28.
- Gorna K, Hund M, Vucak M, Grohn F, Wegner G. Amorphous calcium carbonate in form of spherical nanosized particles and its application as fillers for polymers. *Mater Sci Eng A Struct Mater Prop Microstruct Process.* 2008;477:217–25.
- Bleach NC, Nazhat SN, Tanner KE, Kellomäki M, Törmälä P. Effect of filler content on mechanical and dynamic mechanical properties of particulate biphasic calcium phosphate-poly(lactide) composites. *Biomaterials.* 2002;23:1579–85.
- Pluta M, Murariu M, Alexandre M, Galeski A, Dubois P. Polylactide compositions. The influence of ageing on the structure, thermal and viscoelastic properties of PLA/calcium sulfate composites. *Polym Degrad Stabil.* 2008;93:925–31.

20. Imre B, Keledi G, Renner K, Móczó J, Murariu M, Dubois P, Pukánszky B. Adhesion and micromechanical deformation processes in PLA/CaSO₄ composites. *Carbohydr Polym*. 2012;89:759–67.
21. Liu T, Yu F, Yu X, Zhao X, Lu A, Wang J. Basalt fiber reinforced and elastomer toughened polylactide composites: mechanical properties, rheology, crystallization, and morphology. *J Appl Polym Sci*. 2012;125:1292–301.
22. Shen L, Yang H, Ying J, Qiao F, Peng M. Preparation and mechanical properties of carbon fiber reinforced hydroxyapatite/polylactide biocomposites. *J Mater Sci Mater Med*. 2009;20:2259–65.
23. Plackett D, Logstrupndersen T, Batsberg Pedersen W and Nielsen L. Biodegradable composites based on polylactide and jute fibres. *Compos. Sci. Technol*. 2003;63:1287–96.
24. Tábi T, Sajo IE, Szabó F, Luyt AS, Kovács JG. Crystalline structure of annealed poly(lactic acid) and its relation to processing. *Express Polym Lett*. 2010;4:659–68.
25. Perego G, Cella GD. Mechanical properties. In: Auras R, Lim L-T, Selke SEM, Tsuji H, editors. *Poly(lactic acid): synthesis, structures, properties, processing, and applications*. Hoboken, New Jersey: Wiley; 2010. p. 141–53.
26. Malmgren T, Mays J, Pyda M. Characterization of poly(lactic acid) by size exclusion chromatography, differential refractometry, light scattering and thermal analysis. *J Therm Anal Calorim*. 2006;83:35–40.
27. Day M, Nawaby AV, Liao X. A DSC study of the crystallization behaviour of poly(lactic acid) and its nanocomposites. *J Therm Anal Calorim*. 2006;86:623–9.
28. Molnár K, Móczó J, Murariu M, Dubois P, Pukánszky B. Factors affecting the properties of PLA/CaSO₄ composites: homogeneity and interactions. *Express Polym Lett*. 2009;3:49–61.
29. Chow WS, Lok SK. Thermal properties of poly(lactic acid)/organo-montmorillonite nanocomposites. *J Therm Anal Calorim*. 2009;95:627–32.
30. Shi N, Dou Q. Non-isothermal cold crystallization kinetics of poly(lactic acid)/poly(butylene adipate-co-terephthalate)/treated calcium carbonate composites. *J Therm Anal Calorim*. 2015;119:635–42.
31. Delpouve N, Arnoult M, Saiter A, Dargent E, Saiter J-M. Evidence of two mobile amorphous phases in semicrystalline polylactide observed from calorimetric investigations. *Polym Eng Sci*. 2014;54:1144–50.
32. Harris AM, Lee EC. Improving mechanical performance of injection molded PLA by controlling crystallinity. *J Appl Polym Sci*. 2008;107:2246–55.
33. Kolstad JJ. Crystallization kinetics of poly(L-lactide-co-mesolactide). *J Appl Polym Sci*. 1996;62:1079–91.
34. Tsuji H, Takai H, Fukuda N, Takikawa H. Non-isothermal crystallization behavior of poly(L-lactic acid) in the presence of various additives. *Macromol Mater Eng*. 2006;291:325–35.
35. Pan P, Liang Z, Cao A, Inoue Y. Layered metal phosphonate reinforced poly(L-lactide) composites with a highly enhanced crystallization rate. *ACS Appl Mater Interfaces*. 2009;1:402–11.
36. Qian X, Zhou M, Xu D, Xu SJ, Jin YF. Isothermal and non-isothermal crystallization behavior of poly(L-lactic acid) with nucleating agents. In: Kim YH, Yarlagadda P, Zhang XD, Ai ZJ, editors. *Adv Mater Struct*. 2011; 335–336(Pts 1 and 2):1299–302.
37. Cheng S, Lau K, Liu T, Zhao Y, Lam P-M, Yin Y. Mechanical and thermal properties of chicken feather fiber/PLA green composites. *Compos Part B*. 2009;40:650–4.
38. Fukushima K, Tabuani D, Camino G. Nanocomposites of PLA and PCL based on montmorillonite and sepiolite. *Mater Sci Eng*. 2009;29:1433–41.
39. Picard E, Espuche E, Fulchiron R. Effect of an organo-modified montmorillonite on PLA crystallization and gas barrier properties. *Appl Clay Sci*. 2011;53:58–65.
40. Zhao Y-Q, Cheung H-Y, Lau K-T, Xu C-L, Zhao D-D, Li H-L. Silkworm silk/poly(lactic acid) biocomposites: dynamic mechanical, thermal and biodegradable properties. *Polym Degrad Stab*. 2010;95:1978–87.
41. Anderson KS, Hillmyer MA. Melt preparation and nucleation efficiency of polylactide stereocomplex crystallites. *Polymer*. 2006;47:2030–5.
42. Kulinski Z, Piorkowska E. Crystallization, structure and properties of plasticized poly(L-lactide). *Polymer*. 2005;46:10290–300.
43. Kulinski Z, Piorkowska E, Gadzinowska K, Stasiak M. Plasticization of poly(L-lactide) with poly(propylene glycol). *Biomacromolecules*. 2006;7:2128–35.
44. Piorkowska E, Kulinski Z, Galeski A, Masirek R. Plasticization of semicrystalline poly(L-lactide) with poly(propylene glycol). *Polymer*. 2006;47:7178–88.
45. Arrieta MP, López J, Hernández A, Rayón E. Ternary PLA-PHB-limonene blends intended for biodegradable food packaging applications. *Eur Polym J*. 2014;50:255–70.
46. Pongtanayut K, Thongpin C, Santawitee O. The effect of rubber on morphology, thermal properties and mechanical properties of PLA/NR and PLA/ENR blends. *Energy Proc*. 2013;34:888–97.
47. Abdelwahab MA, Flynn A, Chiou B-S, Imam S, Orts W, Chiellini E. Thermal, mechanical and morphological characterization of plasticized PLA-PHB blends. *Polym Degrad Stab*. 2012;97:1822–8.
48. Jandas PJ, Mohanty S, Nayak SK. Thermal properties and cold crystallization kinetics of surface-treated banana fiber (BF)-reinforced poly(lactic acid) (PLA) nanocomposites. *J Therm Anal Calorim*. 2013;114:1265–78.
49. Chieng B, Ibrahim N, Wan Yunus W, Hussein M, Loo Y. Effect of graphene nanoplatelets as nanofiller in plasticized poly(lactic acid) nanocomposites. *J Therm Anal Calorim*. 2014;118:1551–9.
50. Park JW, Im SS, Kim SH, Kim YH. Biodegradable polymer blends of poly(L-lactic acid) and gelatinized starch. *Polym Eng Sci*. 2000;40:2539–50.
51. Teixeira ED, Curvelo AAS, Correa AC, Marconcini JM, Glenn GM, Mattoso LHC. Properties of thermoplastic starch from cassava bagasse and cassava starch and their blends with poly(lactic acid). *Ind Crop Prod*. 2012;37:61–8.
52. Li H, Huneault MA. Crystallization of PLA/thermoplastic starch blends. *Int Polym Process*. 2008;23:412–8.
53. Li H, Huneault MA. Comparison of sorbitol and glycerol as plasticizers for thermoplastic starch in TPS/PLA blends. *J Appl Polym Sci*. 2011;119:2439–48.
54. Iovino R, Zullo R, Rao MA, Cassar L, Gianfreda L. Biodegradation of poly(lactic acid)/starch/coir biocomposites under controlled composting conditions. *Polym Degrad Stab*. 2008;93:147–57.
55. Sarazin P, Li G, Orts WJ, Favis BD. Binary and ternary blends of polylactide, polycaprolactone and thermoplastic starch. *Polymer*. 2008;49:599–609.
56. Phetwarotai W, Potiyaraj P, Aht-Ong D. Biodegradation of polylactide and gelatinized starch blend films under controlled soil burial conditions. *J Polym Environ*. 2013;21:95–107.
57. Huneault MA, Li H. Morphology and properties of compatibilized polylactide/thermoplastic starch blends. *Polymer*. 2007;48:270–80.
58. Lu DR, Xiao CM, Xu SJ. Starch-based completely biodegradable polymer materials. *Express Polym Lett*. 2009;3:366–75.
59. Kawai T, Rahman N, Matsuba G, Nishida K, Kanaya T, Nakano M, Okamoto H, Kawada J, Usuki A, Honma N, Nakajima K, Matsuda M. Crystallization and melting behavior of poly(L-lactic acid). *Macromolecules*. 2007;40:9463–9.
60. Zhang J, Tashiro K, Tsuji H, Domb AJ. Disorder-to-order phase transition and multiple melting behavior of poly(L-lactide) investigated by simultaneous measurements of WAXD and DSC. *Macromolecules*. 2008;41:1352–7.

61. Pan P, Zhu B, Inoue Y. Enthalpy relaxation and embrittlement of poly(L-lactide) during physical aging. *Macromolecules*. 2007;40:9664–71.
62. Dorgan JR, Janzen J, Clayton MP, Hait SB, Knauss DM. Melt rheology of variable L-content poly(lactic acid). *J Rheol*. 2005;49:607–19.
63. Blomqvist J. RIS Metropolis Monte Carlo studies of poly(L-lactic), poly(L, D-lactic) and polyglycolic acids. *Polymer*. 2001;42:3515–21.
64. Dorgan JR, Janzen J, Knauss DM, Hait SB, Limoges BR, Hutchinson MH. Fundamental solution and single-chain properties of polylactides. *J Polym Sci Part A Polym Phys*. 2005;43:3100–11.